ELSEVIER

Spectrochimica Acta Part B 62 (2007) 325–336

SPECTROCHIMICA ACTA PART B

www.elsevier.com/locate/sab

Calculation of rate constants for asymmetric charge transfer, and their effect on relative sensitivity factors in glow discharge mass spectrometry

Annemie Bogaerts [a,*], Krassimir A. Temelkov [b], Nikolay K. Vuchkov [b], Renaat Gijbels [a]

[a] Research Group PLASMANT, Department of Chemistry, University of Antwerp, Universiteitsplein 1, B-2610 Wilrijk-Antwerp, Belgium
[b] Metal Vapor Lasers Laboratory, Institute of Solid State Physics, Bulgarian Academy of Sciences, 72 Tzarigradsko Chaussee, 1784 Sofia, Bulgaria

Received 21 December 2006; accepted 12 March 2007
Available online 24 March 2007

Abstract

For this paper, we have calculated the rate coefficients for asymmetric charge transfer between Ar^+ ions and all elements of interest in analytical glow discharges, based on a semi-classical approach. These values were then used to make predictions on the relative sensitivity factors (RSFs) in glow discharge mass spectrometry (GDMS) (VG9000 discharge cell) for various elements. The RSFs were calculated based on a transport factor, and an ionization factor, which comprises asymmetric charge transfer, Penning ionization and electron impact ionization. The ionization rates of these three processes were calculated explicitly, based on our earlier computer simulations, in combination with the rate coefficients and cross sections of the ionization processes for different elements. In this way, we are able to offer a rationalization of the experimental RSFs. It is demonstrated that variations in RSFs are largely determined by the occurrence of asymmetric charge transfer in the glow discharge plasma.

Keywords: Asymmetric charge transfer; Relative sensitivity factors; Glow discharge mass spectrometry; Modeling; Rate coefficient; Penning ionization

1. Introduction

Glow discharge mass spectrometry (GDMS) is a sensitive technique, which is used among others for the routine trace analysis of solid conducting materials [1–3]. The sample to be analyzed acts as the cathode of the glow discharge plasma. The technique can also be applied to analyze non-conducting materials, by mixing them with a conducting binding powder, by using a secondary cathode in front of the sample, or by applying rf power. One of the benefits of GDMS is the fairly uniform sensitivity for multi-elemental analysis. The so-called relative sensitivity factors (RSFs) lie generally within one order of magnitude, allowing for standardless semi-quantitative panoramic analysis. The RSF in GDMS is defined as the factor that has to be multiplied with the measured ion current ratio in order to obtain the relative concentration, i.e.:

$$\frac{C_x}{C_s} = \mathrm{RSF}\left[\frac{x}{s}\right] \times \frac{I_x}{I_s} \tag{1}$$

where I and C are the ion current and the concentration, respectively, and x and s represent the element x and the internal standard s, respectively. In this sense, it has actually the meaning of *insensitivity factor*. The *sensitivity* is expressed by the relative ion yield (RIY), which is inversely proportional to the RSF:

$$\mathrm{RSF}\left[\frac{x}{s}\right] = \frac{1}{\mathrm{RIY}\left[\frac{x}{s}\right]} \times \frac{M_x}{M_s} \tag{2}$$

where M_x and M_s denote the atomic masses of element x and standard s.

For obtaining quantitative analytical results, the RSFs of the various elements within a sample need to be known as accurately as possible. This information can be obtained by analyzing certified reference materials, and it appears that the RSFs show minimal matrix-dependence [4–8]. Moreover, variations in RSFs can also be predicted by theoretical models. A number of simplified empirical models, based on fitting parameters to obtain the best agreement between calculated and measured RSFs, have been described in the literature [4,9–11]. These models generally reach a more or less satisfactory agreement

* Corresponding author.
E-mail address: Annemie.Bogaerts@ua.ac.be (A. Bogaerts).

0584-8547/$ - see front matter © 2007 Elsevier B.V. All rights reserved.
doi:10.1016/j.sab.2007.03.010

between theory and experimental values, but they are based on the assumption of some kind of equilibrium in the plasma, which certainly does not exist in glow discharge plasmas. Moreover, by using enough fitting parameters, one can in fact always achieve some agreement with experimental values, but because of their weak theoretical basis, the fitting parameters mostly have no real physical meaning.

The empirical model that describes the physical processes occurring in GDMS in the most realistic way, is the one by Vieth and Huneke, which is based on transport and ionization of the sputtered atoms [4]. However, it is still based on some fitting parameters, which can take arbitrary, physically unrealistic values. Moreover, some discrepancies were observed between experimental and calculated RSFs for certain elements, which could not be explained.

Therefore, we have earlier developed a model [12], based on the ideas of Vieth and Huneke [4], but instead of using fitting parameters, we applied the physical background that we had acquired by our explicit modeling network of glow discharge plasmas (e.g. [13,14]). Based on a list of 45 elements of the periodic table, it was strongly suggested that, besides transport of sputtered atoms, electron impact and Penning ionization, asymmetric charge transfer between sputtered atoms and Ar^+ ions is mainly responsible for the variations in RSFs among different elements [12]. Indeed, in contrast to Penning ionization and electron impact ionization, asymmetric charge transfer between Ar^+ ions and sputtered atoms is found to be a very selective process. It occurs only if the energy difference between the Ar^+ ion ground state (or Ar^+ ion metastable level) and the energy levels of the resulting analyte ion is sufficiently small, and the efficiency of this process generally decreases with growing energy difference between the levels.

To make this clear, Fig. 1 illustrates the experimental RSFs adopted from [4] for the various elements in an argon glow discharge. Recall from the above definition (Eqs. (1) and (2)) that the more efficiently an element is ionized, the lower is its RSF. The elements can roughly be subdivided in three categories. The elements N, O and Cl have a higher ionization potential than the Ar metastable atom level (at 11.55 eV) and hence, cannot be ionized by Penning ionization. Moreover, they have no suitable ionic energy levels available for asymmetric charge transfer with Ar^+ ions. Therefore, they can only be ionized by electron impact ionization, and because the latter process is generally of lower importance than Penning ionization and asymmetric charge transfer [14], these elements are characterized by a high RSF. The second category consists of elements which can undergo both Penning ionization and electron impact ionization, but they have no (or only a few) levels available for asymmetric charge transfer, as was deduced in Ref. [12]. Hence, their RSFs are also quite high (i.e., above 1; this is the RSF by definition of the chosen standard Fe, which has many levels available for asymmetric charge transfer). Finally, the third category comprises the elements which have many ionic levels available for asymmetric charge transfer with Ar^+ ions (see Table 1 of Ref. [12]), and hence, which can be ionized by asymmetric charge transfer, as well as by Penning and electron impact ionization. For this reason, their RSFs are typically low (around 1, hence comparable to Fe, which belongs also to this category).

However, the hypothesis of the role of asymmetric charge transfer in determining variations in RSFs, as also illustrated in Fig. 1, could not yet be confirmed by numerical simulations, due to the lack of data for rate constants of asymmetric charge transfer between Ar^+ ions and most elements of the periodic system. The only evidence was a strong correlation observed between the RSFs and RIYs (or more precisely: the difference between experimental RIYs and predicted values without including asymmetric charge transfer) and the number of levels available for asymmetric charge transfer [12].

It is true that data for asymmetric charge transfer are very scarce in the literature, at least for reactions at thermal energy, between Ar^+ ions and most elements of the periodic table, such as the transition metals, which are of interest for our study. Many papers exist for asymmetric charge transfer at high to very high projectile energies (several tens of eV to the MeV range), both theoretically and experimentally, mainly for rare gases, H, C and the alkali metals (e.g. [15–18]). We are, however, interested in asymmetric charge transfer at thermal energies, because the Ar^+ ions are more or less thermalized in the

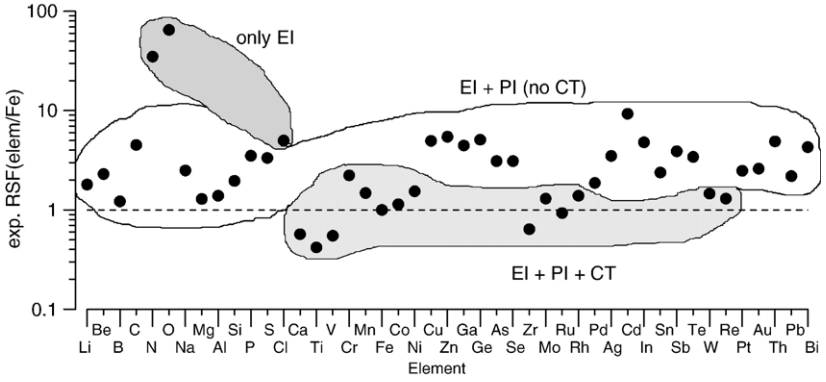

Fig. 1. Experimental RSFs for GDMS in a direct current (dc) argon glow discharge, as obtained from Ref. [4], for various elements of the periodic table, illustrating that the elements can be subdivided into three categories, depending on whether (i) only electron impact ionization (EI) is possible, (ii) both EI and Penning ionization (PI) play a role, and (iii) EI, PI and asymmetric charge transfer (CT) are possible. Note that the higher the ionization efficiency (like in the third category), the lower the RSF.

negative glow region, which constitutes the major part of the glow discharge and the most interesting region for ionization processes.

Experimental data for asymmetric charge transfer cross sections at thermal energies are available in the literature, but most of these data concern reactions of rare gases or molecular gases, such as CO, H_2 and O_2 [19–23]. Concerning asymmetric charge transfer between Ar^+ ions and metal atoms, as is of interest for glow discharges, data are much more limited.

Several papers have shown evidence for the occurrence of asymmetric charge transfer in analytical glow discharges, but without yielding quantitative data on cross sections or rate constants (e.g. [24–42]). For specific combinations of reactants, in connection to metal vapor ion lasers, cross section data are available, such as for He^+–Cd (e.g. [43–45]), He^+–Zn (e.g. [45,46]), He^+–Hg (e.g. [20,47–49]), He^+–Cs (e.g. [50]), Ne^+–Zn (e.g. [51]), Ne^+–Mg (e.g. [45]), Xe^+–Ca,Sr (e.g. [52]), different combinations of He^+, Xe^+ or Cs^+ ions with Fe, Mo, Al, Ti and C atoms [53], and of He^+ or Ne^+ ions with Cu, Ag, Al, Au, Hg, Cd and Zn [54], and finally for He^+–Cu (780.8/740.4 nm), Ne^+–Cu (260.0/252.9 nm and 248.6/270.3 nm), He^+–Ag (800.5 nm), Ne^+–Ag (478.8 nm), and He^+–I (576.1 nm and 658.5 nm) impact couples [55]. However, no systematic data appear to be available for Ar^+ ions and various transition metal atoms, which is mostly relevant for glow discharges, and in particular for our present study on RSFs. It is also dangerous to deduce the cross sections from data between other elements. Indeed, the process seems to be fairly complicated. For instance, it is not always true that the smallest energy difference between energy levels yields the highest cross section [45,46].

In 1973, Turner-Smith et al. [45] presented a formula to calculate cross sections and rate coefficients for asymmetric charge transfer at thermal energy between an arbitrary ion and atom, based on a semi-classical approach. They applied this method for asymmetric charge transfer reactions of He^+ ions with Zn, Cd and Se atoms, and of Ne^+ ions with Mg atoms, as pumping mechanisms for metal vapor ion lasers, as also mentioned above. In 2006, Temelkov et al. [54] applied this formula for reactions in He/Cu, Ne/Cu, He/Ag, Ne/Ag, He/Al, Ne/Al, He/Au, He/Hg, He/Cd and He/Zn mixtures, again of interest for metal vapor ion lasers. However, they used another dependence of the cross section on energy separation between the levels, which yielded better agreement with experiment. Recently, this approach was also used to predict the cross section for charge transfer population of some Cu, Ag and I ion levels, and the theoretical results were in fairly good agreement with experimental cross sections (discrepancy between 3 and 50%) [55].

In the present paper, we will apply the same approach as in Ref. [54] to calculate the rate coefficients for asymmetric charge transfer between Ar^+ ions and atoms of all elements of interest in analytical glow discharges. The calculation method and the results will be presented in the next section. Furthermore, based on these calculated rate coefficients, we will try to calculate the ionization efficiency of all elements, and predict their effect on variations in RSFs. This will be illustrated in Section 3. Finally, a conclusion will be given in Section 4.

2. Calculation of rate coefficients for asymmetric charge transfer

As mentioned above, the formula used to calculate rate coefficients for asymmetric charge transfer is based on the theory of Turner-Smith et al. [45]. The treatment is a semi-classical approach, based on the Landau and Zener curve-crossing formula (see Ref. [45] for more details). The reactions of interest involve a rare gas ion and a metal atom of high polarizability in the initial state, and a metal ion and a rare gas atom of very low polarizability in the final state. Moreover, the energy defect at infinite separation is much larger than the initial kinetic energy. If these conditions are fulfilled, the cross section may be calculated using the following expression:

$$\sigma = \frac{4\pi e}{v_r}\sqrt{\frac{\alpha}{\mu_r}}\exp(-G)[1-\exp(-G)] = \sigma_0 \times \exp(-G)[1-\exp(-G)] \tag{3}$$

Note that this formula is in the CGS system, i.e., $e = 4.8029 \times 10^{-10}$ statcoulomb, v_r is the relative velocity (in cm s^{-1}), α is the metal atom polarizability (in cm^3) and μ_r is the reduced mass (in g). Finally, the parameter G describes the cross section dependence on the infinite separation energy defect, $\Delta(\infty)$, between the levels of the impacting ion (e.g. Ar^+) and the product ion. This dependence can be expressed as [45]:

$$G = \frac{\pi(0.66 I_{gas})^2 e^{3/2}\alpha^{3/4}\mu_r^{1/2}}{\hbar a_0^2(2\Delta(\infty))^{9/4}}\exp\left[-\frac{2^{5/4}(0.86)}{(a_0 e)^{1/2}}\left(\frac{I_{gas}^2\alpha}{\Delta(\infty)}\right)^{1/4}\right] \tag{4}$$

This formula is also in the CGS system, hence the energies (ionization potential of the gas, I_{gas}, and infinite separation energy defect, $\Delta(\infty)$) are in erg, a_0 is the Bohr radius (in cm), Planck's constant h is in erg*s, and the other symbols are explained above. More details about the theory can be found in [45].

Fig. 2(a, b) illustrates how this G value varies as a function of the infinite separation energy defect $\Delta(\infty)$ for asymmetric charge transfer with Ar^+ ions, as calculated with the above formula, for two elements, i.e. Fe (a) and Cu (b). All the other elements exhibit a very similar behavior: the maximum value of G is always between 0.6 and 0.7, and is reached for an energy defect between 0.1 and 0.25 eV.

A reasonable agreement was reached between calculated and measured cross sections for He^+/Cd and Ne^+/Mg, at least for the absolute value of the cross section, but the dependence on the infinite separation energy defect, $\Delta(\infty)$, was less satisfying, both with respect to the optimal energy defect and the shape of the curves (cf. Fig. 3 of Ref. [45]). It was indeed pointed out by several authors [20,56–58] that the curve-crossing model of Turner-Smith and coworkers [45] does not sufficiently reflect the reality. Indeed, it is based on a one-electron model, whereas asymmetric charge transfer is actually a two-electron process, i.e., one valence electron of the atom is transferred to the impacting ion, while the other valence electron is excited to a highly excited level. They further pointed out that molecular

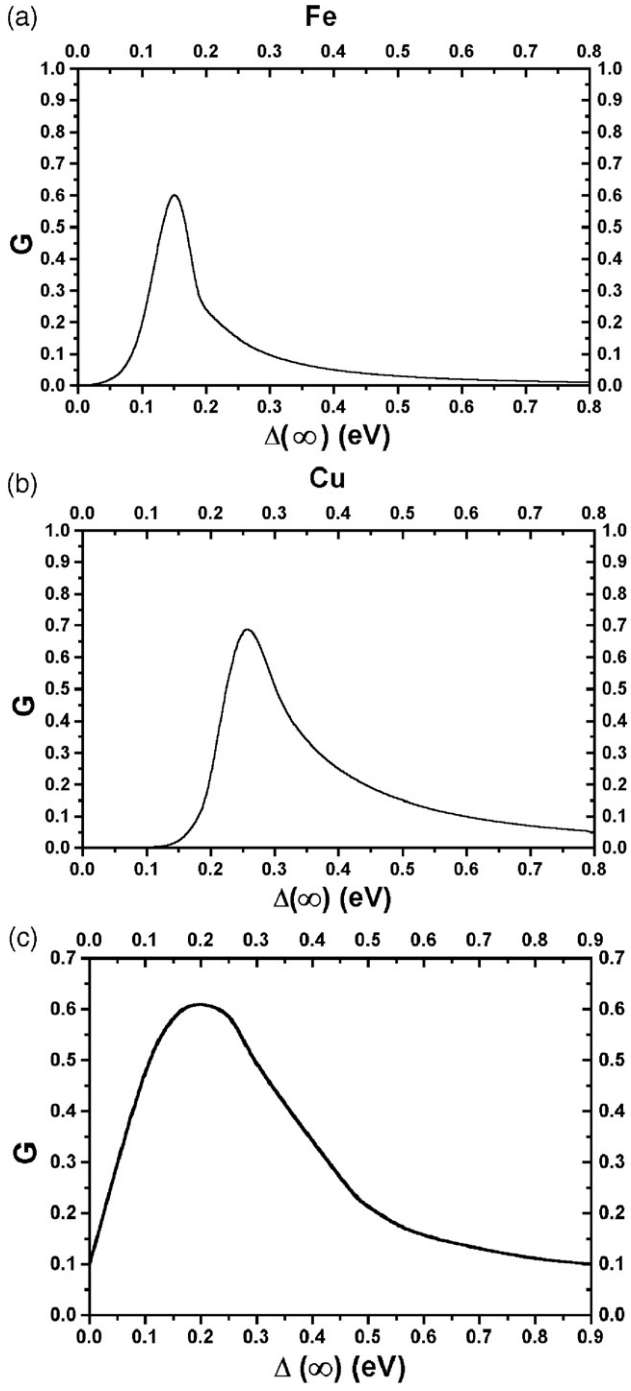

Fig. 2. G factor as a function of the infinite separation energy defect, $\Delta(\infty)$, as calculated with Eq. (2) for Fe (a) and Cu (b), as well as obtained from the experimental energy dependence of the cross section (c) (for more explanation, see text: Section 2, fourth paragraph). $\Delta(\infty)$ is defined as the energy of the Ar^+ ion level minus the energy of the element ionic level. The dependence as illustrated in panel (c) is used in our calculations for the asymmetric charge transfer rate coefficients for all elements.

states need to be involved in the curve crossing. However, they did not suggest any alternative formula for cross section calculations.

Therefore, we decided to circumvent this problem by adopting the dependence of the G parameter on the infinite separation energy defect from experimental data (cf. Fig. 3 of Ref. [45]) instead of from Eq. (4) above, following the approach of Temelkov et al. [54]. This is of course also an approximation, but it proved already to be valid for several impact couples investigated up to now [54,55], i.e. for He^+–Cu, Ne^+–Cu, He^+–Ag, Ne^+–Ag, He^+–Al, Ne^+–Al, He^+–Au, He^+–Hg, He^+–Cd, He^+–Zn [54] and for some specific levels (transitions), i.e., He^+–Cu (780.8/740.4 nm), Ne^+–Cu (260.0/252.9 nm and 248.6/270.3 nm), He^+–Ag (800.5 nm), Ne^+–Ag (478.8 nm), and He^+–I (576.1 nm and 658.5 nm) [55]. This energy dependence is illustrated in Fig. 2(c). It is clear that the G value now yields non-zero values for an energy defect of 0 eV, and also spreads out to higher values of $\Delta(\infty)$, in correlation with the experimental cross section dependence on $\Delta(\infty)$. Hence, instead of using the above Eq. (4) for G as a function of $\Delta(\infty)$, we will apply the dependence illustrated in Fig. 2(c), in order to calculate the asymmetric charge transfer rate coefficients.

The above formula for the charge transfer cross section (Eq. (3)) was applied to all elements, for which ionic levels exist lying close to the Ar^+ ion ground state (or metastable level), as was illustrated in Table 1 of Ref. [12], because these elements can give rise to asymmetric charge transfer with Ar^+ ions. Table 1 of the present paper summarizes the calculation results for σ_0, i.e. the part which is independent of the parameter G. Beside the cross section, also the corresponding rate coefficient ($k=\langle\sigma_0 v_r\rangle$) is presented, in the last column. It is in the order of $1–3\times10^{-9}$ cm^3 s^{-1}, for all elements investigated. However, this value still needs to be multiplied with the G-dependent factor, i.e. $\exp(-G)*(1-\exp(-G))$.

Table 1
Calculation results obtained for the G-independent part of the charge transfer cross section, σ_0, as well as the corresponding rate coefficient: $k=\langle\sigma_0 \cdot v_r\rangle$

Impact couple	α (10^{-23} cm^3)	μ_r (10^{-23} g)	$\sigma_0*\langle T_g\rangle^{-1/2}$ (10^{-12} $cm^2 \cdot K^{-1/2}$)	$k=\langle\sigma_0 v_r\rangle$ (10^{-9} $cm^3 \cdot s^{-1}$)
Ar^+–Ca	0.884	3.322	1.080	3.114
Ar^+–Ti	0.739	3.617	0.987	2.728
Ar^+–V	0.755	3.718	0.998	2.720
Ar^+–Cr	0.375	3.751	0.704	1.909
Ar^+–Mn	0.647	3.841	0.924	2.477
Ar^+–Fe	0.589	3.867	0.881	2.355
Ar^+–Co	0.593	3.954	0.884	2.337
Ar^+–Ni	0.620	3.948	0.905	2.392
Ar^+–Cu	0.305	4.073	0.634	1.650
Ar^+–Zn	0.453	4.117	0.773	2.001
Ar^+–Ge	0.590	4.279	0.883	2.242
Ar^+–Zr	0.738	4.613	0.987	2.414
Ar^+–Mo	0.345	4.683	0.675	1.638
Ar^+–Ru	0.328	4.754	0.658	1.586
Ar^+–Rh	0.321	4.779	0.651	1.565
Ar^+–W	0.579	5.450	0.874	1.967
Ar^+–Re	0.592	5.462	0.883	1.986
Ar^+–Pt	0.243	5.506	0.566	1.267
Ar^+–Au	0.233	5.515	0.554	1.239
Ar^+–Tl	1.328	5.549	1.324	2.953
Ar^+–Pb	1.298	5.561	1.309	2.916
Ar^+–Bi	1.668	5.569	1.483	3.303

The other columns present the data needed to calculate the cross sections and rate coefficients. α is the polarizability of the metal atom, μ_r is the reduced mass of the system, and $\langle T_g\rangle$ is the average gas temperature, which defines the Maxwellian energy distribution of the ions.

This G value has to be determined for each level lying close enough to the Ar^+ ion ground state (or Ar^+ ion metastable level), which is hence available for asymmetric charge transfer. In this respect, we have considered all levels lying up to 0.9 eV below the Ar^+ ion ground state. This is based on the fact that for the He–Se^+ laser 44 laser lines are reported with 15 upper laser levels, populated by asymmetric charge transfer, and the largest energy defect was 0.816 eV [59]. If there are several levels, then the sum of all levels has to be taken. In this way, an element which has many ionic levels lying close to the Ar^+ ion ground state (or metastable level) will result in a larger total G value, and hence in a larger charge transfer rate coefficient.

Table 2 gives an overview, for all elements investigated (i.e. which have energy levels available for asymmetric charge transfer with Ar^+), of the infinite separation energy defects $\Delta(\infty)$, and the corresponding G values, as obtained from Fig. 2(c). The infinite separation energy defects were obtained from the tables of Moore [60]. For most elements, there are several levels available for asymmetric charge transfer, and hence there are several G values calculated. If the element has many ionic levels lying very close to each other, we have lumped them together into a quasi-level; the number between brackets then indicates the number of levels included in this quasi-level. For Cu and Bi, no ionic levels are available for asymmetric charge transfer with the Ar^+ ions in the ground state, but a few levels lie close to the Ar^+ ion metastable level at 15.94 eV, hence the energy defect is given with respect to this level. For Cu, the only level available is the Cu^+ $3d^9$ 4p ($^3P_2$) level, lying at 15.96 eV, hence 0.02 eV above the Ar^+ ion metastable level. However, Steers and Fielding [25] clearly demonstrated the occurrence of asymmetric charge transfer for this level. The extra energy needed (0.02 eV) is probably supplied from the kinetic energy of the colliding species [25]. From Fig. 2(c), no G value is available for negative values of $\Delta(\infty)$. Because we don't know whether a negative $\Delta(\infty)$ gives rise to the same G value as a positive $\Delta(\infty)$, we have indicated two G values in Table 2 for the case of Cu, namely the G value corresponding to the positive $\Delta(\infty)$ of 0.02 eV (i.e., 0.180) and the G value obtained by extrapolation for the negative $\Delta(\infty)$ of 0.02 eV (i.e., 0.055, shown between brackets).

Finally, we have to combine the outcomes of Table 1 (i.e., $k=<\sigma_0 v_r>$) and Table 2 (i.e., $\exp(-G)*(1-\exp(-G))$) for every (quasi-)level, to obtain the asymmetric charge transfer rate

Table 2
Overview for all elements of the infinite separation energy defects $\Delta(\infty)$, and the corresponding G factors, as obtained from the experimental dependence on energy defect illustrated in Fig. 2(c), for all levels that might play a role in asymmetric charge transfer with Ar^+ ions

Impact couple	$\Delta(\infty)$/eV	G	$\Delta(\infty)$/eV	G	$\Delta(\infty)$/eV	G	$\Delta(\infty)$/eV	G	$\Delta(\infty)$/eV	G	$\Delta(\infty)$/eV	G
Ar^+–Ca	0.404	0.334	0.414	0.322	0.624	0.152	0.634	0.148	0.874	0.103	0.884	0.100
Ar^+–Ti	0.365	0.394	0.385	0.361	0.395	0.348	0.415	0.319	0.445	0.276	0.515	0.202
Ar^+–Ti	0.535	0.190	0.545	0.183	0.625	0.150	0.645	0.144	0.785	0.117	0.805	0.112
Ar^+–Ti	0.825	0.110	0.835	0.108	0.845	0.106	0.855	0.105	0.865	0.104	0.875	0.103
Ar^+–V	0.225	0.600	0.315	0.468	0.355	0.406	0.385	0.361	0.475	0.235	0.485	0.223
Ar^+–V	0.575	0.168	0.795	0.112	0.815	0.110	0.835	0.108	0.855	0.105	0.865	0.103
Ar^+–Cr	0.236 (6)	0.597	0.346 (6)	0.419	0.451 (7)	0.267	0.537 (5)	0.185	0.646 (6)	0.143	0.731 (5)	0.125
Ar^+–Cr	0.861 (6)	0.103										
Ar^+–Mn	0.013	0.155	0.023	0.195	0.033	0.235	0.053	0.315	0.063	0.350	0.073	0.395
Ar^+–Mn	0.163	0.600	0.173	0.605	0.193	0.612	0.203	0.610	0.323	0.455	0.333	0.440
Ar^+–Fe	0.113 (7)	0.510	0.219 (7)	0.603	0.312 (7)	0.473	0.374 (2)	0.375	0.454 (2)	0.265		
Ar^+–Co	0.010	0.145	0.286 (2)	0.515	0.305	0.485	0.95	0.1				
Ar^+–Ni	0.857 (2)	0.105										
Ar^+–Cu	(–) 0.02	0.180 (or 0.055)										
Ar^+–Zn	0.244	0.590	0.354	0.410								
Ar^+–Ge	0.135	0.565										
Ar^+–Zr	0.340 (2)	0.430	0.640 (2)	0.145	0.710	0.130	0.750	0.120	0.870	0.105		
Ar^+–Mo	0.074 (2)	0.390	0.185 (7)	0.610	0.371 (3)	0.590	0.474 (5)	0.235	0.567 (4)	0.170	0.677 (7)	0.135
Ar^+–Mo	0.789 (8)	0.115	0.869 (6)	0.103								
Ar^+–Ru	0.050 (4)	0.305	0.163 (5)	0.595	0.259 (5)	0.570	0.333 (4)	0.435	0.447 (5)	0.270	0.548 (4)	0.175
Ar^+–Ru	0.650 (2)	0.145										
Ar^+–Rh	0.075 (3)	0.400	0.228 (3)	0.600	0.355 (1)	0.410	0.435 (2)	0.290	0.595 (7)	0.155	0.700 (4)	0.130
Ar^+–Rh	0.795 (3)	0.110	0.890 (2)	0.102								
Ar^+–W	0.035 (3)	0.245	0.155 (4)	0.560	0.229 (5)	0.600	0.323 (6)	0.455	0.438 (3)	0.285	0.515 (3)	0.200
Ar^+–W	0.600 (2)	0.155	0.720 (8)	0.130	0.808 (3)	0.110	0.913 (4)	0.101				
Ar^+–Re	0.084	0.425	0.108	0.500	0.190	0.610	0.330	0.445	0.380	0.370	0.385	0.360
	0.495	0.215	0.521	0.195	0.528	0.193	0.764	0.120				
Ar^+–Pt	0.115	0.520	0.425	0.300	0.715	0.130						
Ar^+–Au	0.062	0.345	0.512	0.205								
Ar^+–Tl	0.269	0.550										
Ar^+–Pb	0.140	0.570	0.970	<0.1								
Ar^+–Bi	0.02	0.180	0.08	0.410								

Elements which have no such energy levels, are omitted from the table. For some elements, which have many ionic levels available for asymmetric charge transfer lying very close to each other, these levels are lumped together into a quasi-level, and the number of levels included in this quasi-level is indicated between brackets in the columns of $\Delta(\infty)$. For Ar^+–Cu, two different G values are given, depending on whether the energy defect is considered as a positive or a negative value (see text: Section 2: end of third last paragraph).

coefficient for each element into a specific (quasi-)level. The total asymmetric charge transfer rate coefficient is then the sum of all rate coefficients to the individual levels. For the quasi-levels, the rate coefficient should be multiplied with the number of individual levels included in this quasi-level. The resulting total asymmetric charge transfer rate coefficients for all elements, which have suitable energy levels available for asymmetric charge transfer, are summarized in Table 3 (second column). Note that for Cu two different values are given, depending on the G factor used (see above), i.e. the value corresponding to a positive $\Delta(\infty)$ of 0.02 eV (i.e. 0.23×10^{-9} cm^3 s^{-1}), or the value obtained by extrapolation to a negative $\Delta(\infty)$ of 0.02 eV (i.e. 0.084×10^{-9} cm^3 s^{-1}; shown between brackets in Table 3). The elements which possess no suitable energy levels for asymmetric charge transfer, are also included in the table, showing a rate coefficient of zero. Finally, for Cr and Fe two values are given as well; the value between brackets is an adjusted value, as will be explained in detail in Section 3 below.

The obtained rate coefficients now vary over a wider range, i.e., from 8.4×10^{-11} or 2.3×10^{-10} cm^3 s^{-1} for Cu, which has only one level available for charge transfer with the Ar^+ ion in the metastable state (see above) to values in the order of 10^{-8} cm^3 s^{-1}, for elements such as (Cr, Fe,) Mo, Ru and W, which possess (in principle) several levels suitable for asymmetric charge transfer with Ar^+ ions. In the following section, we will apply these rate coefficients, to calculate the ionization efficiency by asymmetric charge transfer, as well as the overall ionization efficiency, in order to investigate the relative role of asymmetric charge transfer. Furthermore, a theoretical value for the RSFs of the various elements in analytical glow discharges will be predicted. Finally, based on the comparison with the experiment, the validity of using the formula given by Eq. (3) will be assessed.

3. Prediction of variations in RSFs, and contribution of different factors

In order to make a prediction for the RSFs (or RIYs), we follow the approach outlined by Vieth and Huneke [4]. This empirical model states that the RIYs in GDMS are, in principle, determined by (i) processes taking place in the glow discharge source, (ii) the ion transmission efficiency through the mass spectrometer, and (iii) the detector sensitivity. The second and third factors were assumed to be element independent, and are set equal to 1. The first factor comprises (i) the sputtering, (ii) the transport of sputtered atoms, (iii) the ionization and recombination, and (iv) the ion extraction into the mass spectrometer. Under steady state conditions, such as in dc GDMS, the sputtering and the ion extraction from a given sample can be also assumed to be element independent, so that only the transport and the ionization/recombination effects remain [4]:

$$\mathrm{RIY}\left[\frac{x}{s}\right] = S_T\left[\frac{x}{s}\right]\times S_I\left[\frac{x}{s}\right] \quad (5)$$

where S_T and S_I denote the relative efficiencies (of element x versus standard s) of transport and ionization/recombination, respectively.

Table 3
Rate coefficients for asymmetric charge transfer with Ar^+ ions, for all elements having suitable energy levels available, calculated by combining the outcomes of Table 1 (i.e., $k=<\sigma_0 v_r>$) and Table 2 (i.e., $\exp(-G)*(1-\exp(-G))$) for every (quasi-)level

Element	k_{aCT} (10^{-9} cm^3 s^{-1})	k_{PI} (10^{-10} cm^3 s^{-1})	σ_{EI} (at 500 eV) (10^{-16} cm^2)
Li	–	2.97	0.57
Be	–	2.08	0.61
B	–	1.60	0.55
C	–	1.51	0.58
Na	–	3.83	0.86
Mg	–	3.05	0.88
Al	–	2.63	0.82
Si	–	2.16	0.85
P	–	2.00	0.83
S	–	1.97	1.13
Ca	2.54	3.96	1.22
Ti	6.61	2.75	1.18
V	4.98	2.52	1.30
Cr	12.47 (0.62)	2.38	1.33
Mn	6.22	2.31	1.90
Fe	13.76 (3.44)	2.33	1.77
Co	2.15	2.31	1.85
Ni	0.43	2.30	1.94
Cu	0.23 (0.084)	2.36	1.85
Zn	0.94	2.56	1.17
Ga	–	2.51	1.06
Ge	0.55	2.60	1.01
As	–	2.31	1.02
Se	–	2.14	1.21
Zr	2.38	3.03	1.23
Mo	10.40	2.61	1.33
Ru	9.25	2.48	1.65
Rh	5.87	2.46	1.72
Pd	–	2.55	3.48
Ag	–	2.70	1.63
Cd	–	2.87	1.22
In	–	2.98	1.42
Sn	–	3.00	1.18
Sb	–	3.08	1.23
Te	–	2.71	1.43
W	13.48	2.63	1.24
Re	1.09	2.56	1.67
Pt	0.68	2.58	1.66
Au	0.44	2.69	1.64
Tl	0.72	3.30	1.19
Pb	0.97	3.39	0.96
Bi	1.19	3.58	1.20

Note that the total rate coefficient is the sum of all rate coefficients to the individual (quasi-)levels. For Cu, two different values are given, depending on the G factor used (see text). For Cr and Fe, adjusted values are given between brackets, obtained after comparison of theoretically predicted RSFs with experimental values (see discussion with respect to Table 4 below). Also included in the table are the calculated rate coefficients for Penning ionization and the cross sections for electron impact ionization, at an electron energy of 500 eV, for all elements, including the ones that have no suitable energy levels available for asymmetric charge transfer (such as Li, Be, B, etc). Note that for the latter elements, no charge transfer rate coefficients were calculated, as the values are assumed to be zero.

We have adopted the same transport factor as in the model by Vieth and Huneke, i.e. transport occurs by diffusion, and atoms with a higher diffusion coefficient will diffuse more quickly

towards the walls, where they will be lost, so that their concentration in the plasma will be less. (This assumption would not be true for discharge cells based on the "fast flow" concept [61].) Hence, the transport efficiency for the VG9000 discharge cell is inversely proportional to the diffusion coefficient:

$$S_T\left[\frac{x}{s}\right] = \frac{D_s}{D_x} = \frac{(r_{Ar}+r_x)^2\sqrt{\mu_{x-Ar}}}{(r_{Ar}+r_s)^2\sqrt{\mu_{s-Ar}}} \quad (6)$$

Indeed, the diffusion coefficient of atoms of element x in Ar gas is given by: $D_x \propto 1/[(r_{Ar}+r_x)^2\sqrt{\mu_{x-Ar}}]$ [62], where μ_{x-Ar} is the reduced mass of atoms x and argon, and r is the atomic radius.

The ionization/recombination factor (S_I) was assumed in Ref. [4] to be determined by Penning ionization and electron impact ionization, on one hand, and by three-body recombination, on the other hand. However, because the authors did not know any values for the densities of electrons and Ar metastable atoms, they used three fitting parameters, in order to estimate the rates of ionization and recombination. These fitting parameters can, however, easily take physically unrealistic values. Therefore, we use another, more explicit and quantitative approach.

Indeed, based on the results obtained with our modeling network for analytical glow discharges developed earlier (e.g. [13,14]), we know that sputtered elements can be ionized by (i) asymmetric charge transfer with Ar^+ ions, (ii) Penning ionization with Ar metastable atoms (Ar_m^*), and (iii) electron impact ionization [14]. The rates of these three processes can be expressed as follows:

$$\text{Asymmetric charge transfer}: Ar^+ + M \rightarrow Ar^0 + M^{+*}$$
$$\text{Rate} = k_{aCT} \times n_{Ar^+} \times n_M$$

$$\text{Penning ionization}: Ar_m^* + M \rightarrow Ar^0 + M^+ + e^-$$
$$\text{Rate} = k_{PI} \times n_{Ar_m^*} \times n_M$$

$$\text{Electron impact ionization}: e^- + M \rightarrow 2e^- + M^+$$
$$\text{Rate} = \int_{E_{thresh}}^{\infty} \sigma_{EI}(E) \times j_e(E)\,dE \times n_M$$

Note that for electron impact ionization, the energy-dependent cross section is used, instead of a thermal rate coefficient (like for asymmetric charge transfer and Penning ionization) and we must integrate the product of cross section ($\sigma(E)$) and electron flux energy distribution ($j_e(E)$) over all energies, starting from the threshold of electron impact ionization. Furthermore, it followed from our computer simulations that in dc glow discharges electron–ion recombination is negligible compared to ionization [63].

Therefore, returning to the formula for calculating RIYs, we can obtain the ionization efficiency of an element (x), with respect to an internal standard (s), by calculating the sum of the asymmetric charge transfer, Penning ionization and electron impact ionization rates, and dividing by the total ionization rate for the internal standard:

$$S_I\left[\frac{x}{s}\right] = \frac{\text{Rate}(x)}{\text{Rate}(s)} = \frac{\int_{\text{discharge}}\left[(k_{aCT,x}\times n_{Ar^+}) + (k_{PI,x}\times n_{Ar_m^*}) + \left(\int_{E_{thresh}}^{\infty}\sigma_{EI,x}(E)\times j_e(E)dE\right)\right]\times n_x}{\int_{\text{discharge}}\left[(k_{aCT,s}\times n_{Ar^+}) + (k_{PI,s}\times n_{Ar_m^*}) + \left(\int_{E_{thresh}}^{\infty}\sigma_{EI,s}(E)\times j_e(E)dE\right)\right]\times n_s} \quad (7)$$

We have chosen Fe as the internal standard (s), as is common in defining RSFs in GDMS. The above formula is applied to all elements investigated in Ref. [12], i.e. including also the elements which cannot be ionized by asymmetric charge transfer. The number densities of Ar^+ ions and Ar_m^* metastable atoms (n_{Ar^+} and $n_{Ar_m^*}$) and the electron flux energy distributions ($j_e(E)$) are adopted from our modeling calculations [13,14,64]. Note that the densities and flux energy distributions have to be adopted as a function of position in the discharge, and the final product is integrated over the entire discharge region, to obtain the overall ionization efficiency.

The rate coefficients for asymmetric charge transfer (k_{aCT}) were obtained in Section 2 above. The Penning ionization rate coefficients were calculated based on an empirical formula for the cross section [65]: $\sigma_{PI}=(0.0153\mu^{1/2}\pi R_0^3)\times 10^{-15}$ cm^2, where μ is the reduced mass, given in amu, and R_0 denotes the atomic radius (in Å). The rate coefficient can then be obtained as explained above for asymmetric charge transfer (cf. last column of Table 1). The electron impact ionization cross sections for all the elements were estimated by the method of Vriens, as explained in Ref. [66]. The rate coefficients for Penning ionization and the electron impact ionization cross sections at an electron energy of 500 eV are also included in Table 3, for all elements investigated (i.e. for which experimental RSFs were available [4,12]). The electron energy value of 500 eV might seem too high to be representative, but in fact, it corresponds to the fast electron population, which is exactly responsible for ionization and excitation, and this value was indeed calculated by our hybrid modeling network, for the same conditions as under study in the present paper (see Fig. 7 of [13]), and at the same region in the plasma where electron impact ionization of the sputtered atoms reaches its maximum (see Fig. 10 of [14]). It is clear that both the Penning ionization rate coefficients and the electron impact ionization cross sections exhibit less variations among the different elements compared to the asymmetric charge transfer rate coefficients. Indeed, electron impact ionization and Penning ionization can be considered as relatively unselective processes, as long as the ionization potential of the element to be ionized is lower than the electron energy, or the Ar metastable level (11.55 eV), respectively. This is the case for most elements of the periodic table (at least for the elements included in this study; for N, O and Cl, for instance, the ionization potential is higher than the Ar metastable energy, and hence Penning ionization is not possible, which is reflected in much higher RSFs, as was discussed already in Ref. [12] and illustrated in Fig. 1 above). Furthermore, it appears from Table 3 that the rate coefficients for asymmetric charge transfer are generally higher

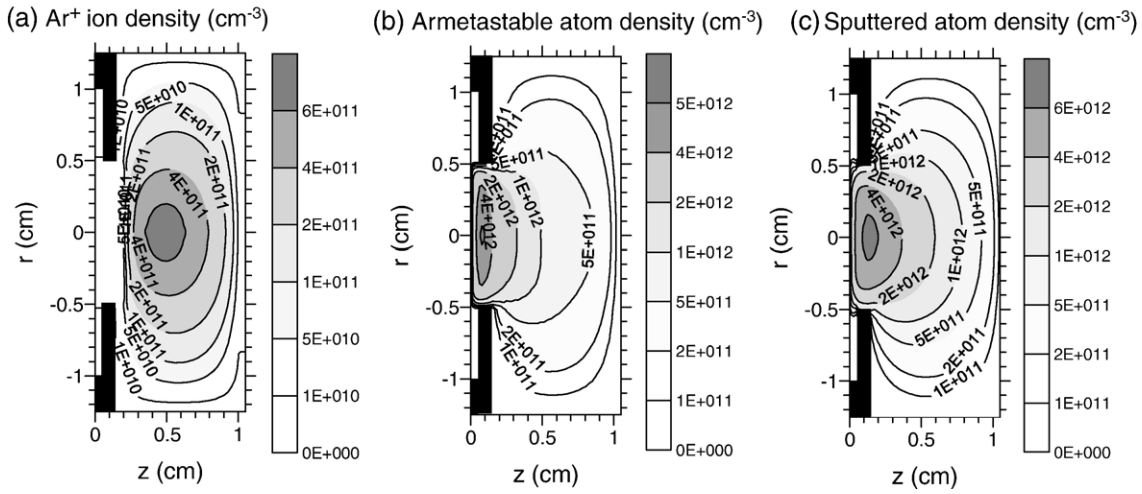

Fig. 3. Density profiles of the Ar^+ ions (a), Ar metastable atoms (b) and sputtered atoms (c), as obtained from our computer simulations [14,63], for typical VG9000 (dc) glow discharge conditions, i.e., 75 Pa argon gas pressure, 1000 V discharge voltage and 3 mA electrical current.

than the Penning ionization rate coefficients, if the elements of course possess suitable ionic energy levels for asymmetric charge transfer to occur. However, the relative importance of asymmetric charge transfer vs. Penning ionization depends not only on the values of their rate coefficients, but also on the densities for Ar^+ ions and Ar metastable atoms.

These density profiles, as well as the sputtered atom density profile, are illustrated in Fig. 3, for typical conditions of the VG9000 glow discharge mass spectrometer, for which the experimental RSFs were obtained [4]. It is clear that the Ar metastable atoms exhibit a higher density than the Ar^+ ions. Note that the Ar metastable density reflects here the sum of the four $3p^5$ 4s levels, i.e. two metastable and two resonant levels, which all have a high density, and can give rise to Penning ionization [67]. Moreover, Fig. 3 illustrates that the spatial overlap between the Ar metastable atom and sputtered atom densities, which also defines the efficiency of the ionization process, is much better than for the Ar^+ ion and sputtered atom density profiles.

Table 4 summarizes for all elements investigated the calculated total ionization rates, obtained by integration over the entire discharge cell (column 2), as well as the relative contributions of asymmetric charge transfer (column 3) and Penning ionization (column 4). The relative contribution of electron impact ionization was always in the order of a few %, as was also predicted by all our previous calculations (e.g. [14,63]), and is therefore left out of the table, in order not to further complicate the story. For the same reason, the elements N, O and Cl, which can only be ionized by electron impact ionization (see Fig. 1 above) are not included in the table.

It appears from this table that the elements can roughly be subdivided in four categories, based on the calculated relative contributions of Penning ionization and asymmetric charge transfer. For the elements which possess (in principle) many ionic energy levels suitable for asymmetric charge transfer (such as Ti, V, Cr, Mn, Fe, Mo, Ru, Rh and W; cf. Table 2), the latter process appears to be the dominant ionization mechanism, with a relative contribution predicted to be about 74–89%. Note, however, that for Cr and Fe also some lower values are given between brackets, which are obtained after reducing the charge transfer rate coefficient, as will be explained in detail below. The elements which possess several suitable energy levels, such as Ca (6 levels; cf. Table 2), Co (5 levels) and Zr (7 levels), appear to be characterized by a contribution of asymmetric charge transfer in the order of 50–60%. The elements which have only one or a few levels available for asymmetric charge transfer (such as Ni, Cu, Zn, Ge, Re, Pt, Au, Tl, Pb and Bi; cf. Table 2), are predominantly ionized by Penning ionization, with a predicted contribution in the order of 60–80%. Finally, the last category consists of the elements which have no suitable energy levels for asymmetric charge transfer, and which only are ionized by Penning ionization (besides a few % of electron impact ionization).

The final aim of our study was to predict variations in the RSFs for various elements. Therefore, column 5 of Table 4 shows the total ionization factor, as calculated by dividing the total ionization rate of element x, by the total ionization rate of Fe (i.e. Eq. (7) above). Combining this ionization factor with the transport factor (which is calculated with Eq. (6) and illustrated in column 6), yields the RIYs (column 7, calculated with Eq. (5)) and the corresponding RSFs for all elements (column 8; calculated with Eq. (2)). The theoretically predicted RSFs can be compared with experimental values, as obtained from Ref. [4] and depicted in column 9.

It is clear that the variations in calculated RSFs are too large, in comparison with the experimental values. Moreover, the calculated values are all larger than 1, except for the assumed standard Fe, which has an RSF of 1 by definition. This suggests that all elements are less efficiently ionized (or transported) than Fe. The transport factor varies only slightly for the different elements, increasing with atomic mass and radius of the elements, with Fe having intermediate values, so this cannot be the reason of the discrepancy. The real reason is the high ionization rate of Fe (calculated to be 8.4×10^{15} s^{-1}, which is the highest of all elements investigated; see column 2), attributed to the high rate coefficient of asymmetric charge transfer (cf. Table 3). This

Table 4
Overview for all elements of the total ionization rate, obtained by integration over the entire discharge region ($R_{ion,tot}$; column 2), the relative contributions of asymmetric charge transfer (aCT; column 3) and Penning ionization (PI; column 4), the ionization and transport factor with respect to the standard s (S_I and S_T; column 5 and 6; taking Fe as the internal standard), the theoretical RIY and RSF (column 7 and 8), the experimental RSF (column 9) and the adjusted RSF, after reducing the asymmetric charge transfer rate coefficients of Fe and Cr (column 10; see text: Section 3: second and third last paragraph)

Element	$R_{ion,tot}$ (s^{-1})	% aCT	% PI	$S_I[x/s]$	$S_T[x/s]$	RIY$[x/s]$	RSF$[x/s]$	RSF_{exp}	$RSF_{adjusted}$
Li	1.0×10^{15}	0	98	0.12 (0.38)	0.61	0.07 (0.23)	1.68	1.8	0.54
Be	7.1×10^{14}	0	98	0.09 (0.26)	0.52	0.04 (0.14)	3.65	2.3	1.17
B	5.5×10^{14}	0	98	0.07 (0.20)	0.45	0.03 (0.09)	6.58	1.22	2.12
C	5.2×10^{14}	0	98	0.06 (0.19)	0.45	0.03 (0.09)	7.74	4.51	2.49
Na	1.3×10^{15}	0	98	0.16 (0.49)	1.15	0.18 (0.56)	2.29	2.5	0.74
Mg	1.1×10^{15}	0	98	0.12 (0.39)	0.99	0.12 (0.38)	3.53	1.29	1.13
Al	9.0×10^{14}	0	98	0.11 (0.33)	0.91	0.10 (0.30)	4.94	1.39	1.59
Si	7.4×10^{14}	0	98	0.09 (0.27)	0.79	0.07 (0.22)	7.21	1.96	2.32
P	6.9×10^{14}	0	98	0.08 (0.25)	0.77	0.06 (0.20)	8.81	3.51	2.83
S	6.8×10^{14}	0	98	0.08 (0.25)	0.77	0.06 (0.19)	9.26	3.34	2.98
Ca	2.8×10^{15}	49	48	0.33 (1.02)	1.39	0.46 (1.42)	1.57	0.57	0.50
Ti	4.6×10^{15}	78	19	0.55 (1.70)	1.10	0.60 (1.87)	1.42	0.42	0.46
V	3.6×10^{15}	74	23	0.43 (1.34)	1.04	0.45 (1.39)	2.04	0.55	0.66
Cr	7.7×10^{15} (1.2×10^{15})	88 (29)	9 (68)	0.92 (0.43)	1.00	0.92 (0.43)	1.01	2.23	2.17
Mn	4.2×10^{15}	79	18	0.50 (1.57)	0.99	0.50 (1.55)	1.97	1.48	0.63
Fe	8.4×10^{15} (2.7×10^{15})	89 (69)	8 (28)	1.00 (1.00)	1.00	1.00 (1.00)	1.0	1.0	1.0
Co	2.0×10^{15}	58	39	0.24 (0.73)	1.01	0.24 (0.74)	4.43	1.14	1.43
Ni	1.7×10^{15}	12	85	0.20 (0.63)	1.00	0.20 (0.63)	5.15	1.54	1.66
Cu	8.6×10^{14}	5	92	0.11 (0.32)	1.04	0.11 (0.33)	10.1	4.96	3.45
Zn	1.4×10^{15}	36	61	0.17 (0.52)	1.11	0.18 (0.57)	6.33	5.46	2.04
Ga	8.6×10^{14}	0	98	0.10 (0.32)	1.10	0.12 (0.35)	11.1	4.45	3.56
Ge	1.2×10^{15}	24	73	0.14 (0.44)	1.14	0.16 (0.50)	8.00	5.1	2.58
As	7.9×10^{14}	0	98	0.09 (0.29)	1.05	0.10 (0.31)	13.5	3.1	4.35
Se	7.3×10^{14}	0	97	0.09 (0.27)	1.00	0.09 (0.27)	16.2	3.1	5.20
Zr	2.4×10^{15}	54	43	0.28 (0.87)	1.34	0.38 (1.17)	4.35	0.64	1.40
Mo	6.6×10^{15}	85	12	0.79 (2.46)	1.20	0.95 (2.95)	1.81	1.3	0.58
Ru	6.0×10^{15}	84	13	0.71 (2.21)	1.16	0.82 (2.56)	2.20	0.93	0.71
Rh	4.1×10^{15}	78	19	0.49 (1.51)	1.18	0.57 (1.78)	3.21	1.39	1.03
Pd	8.8×10^{14}	0	96	0.10 (0.32)	1.20	0.13 (0.39)	15.2	1.87	4.90
Ag	9.3×10^{14}	0	97	0.11 (0.34)	1.25	0.14 (0.43)	14.0	3.5	4.50
Cd	9.8×10^{14}	0	97	0.12 (0.37)	1.32	0.15 (0.48)	13.0	9.3	4.18
In	1.0×10^{15}	0	97	0.12 (0.38)	1.36	0.17 (0.51)	12.4	4.8	3.99
Sn	1.0×10^{15}	0	97	0.12 (0.38)	1.38	0.17 (0.53)	12.6	2.38	4.04
Sb	1.1×10^{15}	0	97	0.13 (0.39)	1.40	0.18 (0.55)	12.4	3.9	3.98
Te	9.3×10^{14}	0	97	0.11 (0.34)	1.28	0.14 (0.44)	16.1	3.42	5.18
W	8.3×10^{15}	87	10	0.99 (3.09)	1.30	1.29 (4.02)	2.55	1.46	0.82
Re	1.5×10^{15}	39	57	0.18 (0.55)	1.28	0.23 (0.70)	14.8	1.3	4.75
Pt	1.3×10^{15}	28	68	0.15 (0.47)	1.29	0.19 (0.60)	18.0	2.48	5.80
Au	1.2×10^{15}	19	77	0.14 (0.43)	1.33	0.18 (0.57)	19.1	2.6	6.14
Tl	1.5×10^{15}	24	73	0.18 (0.57)	1.56	0.28 (0.88)	12.9	4.9	4.14
Pb	1.7×10^{15}	30	67	0.20 (0.63)	1.59	0.32 (1.00)	11.5	2.19	3.71
Bi	1.9×10^{15}	33	64	0.22 (0.70)	1.66	0.37 (1.16)	10.0	4.29	3.23

The adjusted values for the total ionization rate, relative contributions of asymmetric charge transfer and Penning ionization, for Fe and Cr, are also given in the table (columns 2, 3 and 4: values between brackets), as well as the adjusted values for the ionization factor and theoretical RIYs for all elements (columns 5 and 7: values between brackets). For Cu, the calculations were made based on the lowest charge transfer rate coefficient (i.e. 8.4×10^{-11} cm^3 s^{-1}), because this yielded a slightly better agreement with the experimental RSF (for comparison: the higher rate coefficient of 2.3×10^{-10} cm^3 s^{-1} yielded an RSF of 3.15).

poses the question whether asymmetric charge transfer is really so significant for Fe, or whether our calculation method overestimates its rate coefficient.

It is true that Fe possesses many ionic energy levels that are energetically available for asymmetric charge transfer with Ar^+ ions (see Table 2). It was also found experimentally by Steers and Thorne [28] (using a microwave boosted source) and by Wagatsuma and Hirokawa [29] that asymmetric charge transfer between Ar^+ ions and Fe atoms takes place in a Grimm-type glow discharge. On the other hand, Hudson et al. [27] have measured the relative populations of 232 excited levels of Fe^+ ions in a hollow cathode discharge in neon and in argon. It was demonstrated that asymmetric charge transfer was indeed responsible for most of the excited Fe^+ population. However, the cross section appeared to be much higher when the excited Fe^+ final level had the same $3d^6$ (^5D) core configuration as the initial Fe atom ground level. There exist many of these levels near the Ne^+ ground state, but no levels are present near the Ar^+ ground state or excited level [27]. For this reason, it was argued that the neon HCD will produce a much brighter FeII spectrum than the argon HCD for all lines originating from levels excited by asymmetric charge transfer. We have checked these

observations, and indeed, it followed from [60] that only the 4p levels around 12.7–13.8 eV (total excitation + ionization energy) have this $3d^6$ (a ^5D) core configuration, but their energy is too low for asymmetric charge transfer with Ar^+ ions to occur. This could indicate that asymmetric charge transfer between Fe and Ar^+ is possible, based on energy considerations only, as also demonstrated in [27–29], but that the rate coefficient is lower than predicted with Eq. (1) above, due to the change in core configuration. To take this assumption at least qualitatively into account, we have repeated the calculations for Fe, by lowering the asymmetric charge transfer rate coefficient by a factor of 4. This is indicated with the values between brackets in Table 4. Note that this factor 4 was chosen, because it yielded reasonable agreement with experimental RSFs (see below), but there is *no firm physical reason* behind this value. This is of course the weakest point of the present calculations, although the fact that we have lowered the rate coefficient for asymmetric charge transfer does have at least some physical basis, and can be justified by the literature (see above). In the future, we hope to refine this adjustment, if the rate coefficients for asymmetric charge transfer could also be measured experimentally, or if some higher level quantum-mechanical calculations could be used, which include effects such as changes in core configuration, and to introduce these data in our glow discharge model.

A similar remark (and adjustment) has to be made for asymmetric charge transfer between Ar^+ ions and Cr atoms. Indeed, Cr appears to have many ionic energy levels available for asymmetric charge transfer, solely based on energy considerations. However, using a glow discharge with and without microwave boosting, Steers and Thorne [28] could not detect any instances of asymmetric charge transfer between Ar^+ and Cr. Indeed, it was argued that this was consistent with the fact that charge transfer can only take place when total electron spin is conserved, and this is only possible for Cr^+ excited levels lying too far away from the Ar^+ ion ground state energy [28]. Since such detailed arguments are not included in the Turner-Smith model, we could not but lower the calculated asymmetric charge transfer rate coefficient for Ar^+/Cr arbitrarily by a factor of 20, and repeated the calculations for Cr. This is also indicated in Table 4 (values between brackets). The factor 20 is chosen because this value yielded reasonable agreement with experimental RSFs. Again, this value of 20 has no firm physical basis, except for the fact that, indeed, we expect the adjustment to be higher for Ar^+/Cr than for Ar^+/Fe, based on observations by Steers and Thorne [28].

Naturally, the adjustment made for the asymmetric charge transfer rate coefficient of Fe affects the theoretically predicted RIYs and RSFs for all elements, as Fe is (typically) chosen as the internal standard. Therefore, column 10 illustrates the new theoretical RSFs, obtained with the adjusted charge transfer rate coefficient for Ar^+/Fe. It is clear that they are now in better agreement with the experimental data. They are, however, sometimes still off by a factor of 2–3, as is also illustrated in Fig. 4. The scatter of data points in Fig. 4 demonstrates that the theory is not yet good enough to have predictive power for the RSFs. This illustrates that the asymmetric charge transfer rate coefficient calculations still need some refinement: by quantum-mechanical approaches or by experiments, including detailed spectroscopic observations and interpretation, not only for Fe and Cr, but in fact for all elements of interest. Moreover, the real processes taking place in the glow discharge plasma are probably more complicated than can be predicted with only an ionization and a (simplified) transport factor. In general, however, the correlation can be considered as reasonable, certainly taking into account that the measured RSFs are also subject to uncertainties (e.g., standard reference materials with certified trace element concentrations, for many elements, are not easily available), and that the RSFs are obtained based on the real physical processes occurring in the glow discharge plasma, and not by using (unphysical) fitting parameters. The most important message from this table is that elements which possess many suitable energy levels for asymmetric charge transfer with Ar^+, and therefore are characterized by high rate coefficients for this process, exhibit low RSFs, whereas elements which have no suitable energy levels available, exhibit much higher RSFs (see also Fig. 1 above). This demonstrates the important role of asymmetric charge transfer in determining the variations in RSFs.

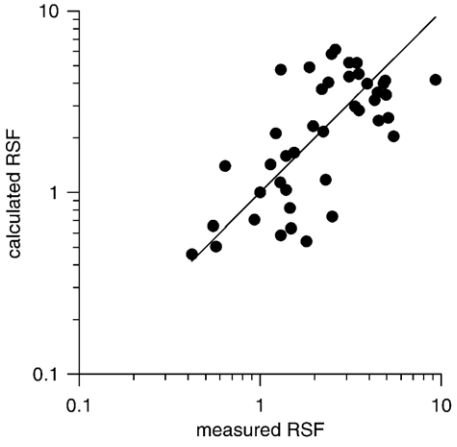

Fig. 4. Calculated vs. experimental RSFs, for all elements investigated (see Table 4).

4. Conclusion

In this paper, we have calculated the rate coefficients for asymmetric charge transfer between Ar^+ ions and atoms of all elements of interest in analytical glow discharges, based on a semi-classical approach [45], where the dependence on the infinite separation energy defect between the ionic levels is taken from the experiment [54,55]. Furthermore, based on these rate coefficients, we have made predictions for variations in RSFs in GDMS for various elements.

The RSFs were calculated following the approach of Vieth and Huneke [4], i.e. based on a transport factor and an ionization factor. The latter is described more explicitly than in the Vieth and Huneke model; it is based on asymmetric charge transfer, Penning ionization and electron impact ionization, and the rates of these processes are calculated explicitly from the

densities and fluxes of the collision partners, obtained from computer simulations of the glow discharge, in combination with the rate coefficients and cross sections of these processes for various elements.

In order to reach reasonable agreement with experimental RSFs, it was argued that the calculated rate coefficients for asymmetric charge transfer of Ar^+ with Fe and with Cr had to be reduced by a certain factor. The latter could be explained, based on arguments in the literature, by the fact that the efficiency of asymmetric charge transfer does not solely depend on energetic considerations (i.e., availability of energy levels), but also on conservation of core configuration [27] and/or total electron spin [28]. This demonstrates that the semi-classical approach of Turner-Smith [45] is only an approximation.

Nevertheless, based on these rate coefficient calculations, and using the physical background that we have acquired in previous years by our explicit modeling work on glow discharges, we are able to offer a rationalization of the experimental RSFs. It is demonstrated that the RSFs are determined by transport of the sputtered atoms in the glow discharge, as well as by Penning ionization (and electron impact ionization to some extent) and by asymmetric charge transfer. Especially the latter process is important, because it is a very selective process, occurring only when the element has suitable ionic energy levels available for asymmetric charge transfer. This conclusion was also drawn in our previous paper [12], but now we were able to go one step further, as we could explicitly calculate the ionization rate by asymmetric charge transfer, by means of the computed rate coefficients.

The only weak point of these calculations is, however, the adjustment factors that we had to apply for the charge transfer rate coefficients of Ar^+ with Fe and Cr atoms. In the future, we hope that rate coefficients for asymmetric charge transfer of Ar^+ ions with atoms of various elements of interest could be measured experimentally or calculated by a quantum-mechanical approach, in order to further assess the validity of the calculation method used (Eq. (3)), and to further refine the predictions on variations in RSFs. Such experimental measurements are in fact included in the experimental programme of the recently approved EC Marie Curie Research Training Network on Analytical Glow Discharges (GLADNET).

Finally, it is worth to mention that the model to predict variations in RSFs can of course still be further refined. Indeed, up to now, we have dealt exclusively with asymmetric charge transfer from Ar^+ ions. However, depending on the discharge conditions and geometries, analyte ions may also be quite abundant. Therefore, asymmetric charge transfer between analyte ions may possibly also play a role in the observed RSFs, if the energy difference between energy levels of both analyte ions is sufficiently small. This might be an explanation for matrix effects between alloys of different base metal compositions.

References

[1] R.K. Marcus (Ed.), Glow Discharge Spectroscopies, Plenum Press, New York, 1993.

[2] R.K. Marcus, J.A.C. Broekaert (Eds.), Glow Discharge Plasmas in Analytical Spectroscopy, Wiley, Chichester, 2003.

[3] N. Jakubowski, A. Bogaerts, V. Hoffmann, Glow discharges in emission and mass spectrometry, in: M. Cullen (Ed.), Atomic Spectroscopy in Elemental Analysis, Blackwell Publishing, Sheffield, 2003.

[4] W. Vieth, J.C. Huneke, Relative sensitivity factors in glow discharge mass spectrometry, Spectrochim. Acta Part B 46 (1991) 137–153.

[5] C. Venzago, M. Weigert, Application of the glow discharge mass spectrometry (GDMS) for the multi-element trace and ultratrace analysis of sputtering targets, Fresenius' J. Anal. Chem. 350 (1994) 303–309.

[6] M. Saito, A contribution to the study of matrix effects in the analysis of solid samples by DC glow discharge mass spectrometry, Spectrochim. Acta Part B 50 (1995) 171–178.

[7] M. Saito, Relative sensitivity factors in direct current glow discharge mass spectrometry using Kr and Xe gas — estimation of the role of Penning ionization, Fresenius' J. Anal. Chem. 351 (1995) 148–153.

[8] M. Saito, The relationship between relative sensitivity factors and ionization potential in dc glow discharge mass spectrometry using Ar/0.2 vol.% H_2 mixture, Anal. Chim. Acta 355 (1997) 129–134.

[9] G.I. Ramendik, D.A. Tyurin, Yu.I. Babikov, Is a universal model for ion formation during mass spectrometric elemental analysis possible? Anal. Chem. 62 (1990) 2501–2503.

[10] R.W. Smithwick III, Theoretical calculations of relative ion yields for glow discharge mass spectrometry, J. Am. Soc. Mass Spectrom. 3 (1992) 79–84.

[11] R.W. Smithwick III, D.W. Lynch, J.C. Franklin, Relative ion yields measured with a high-resolution glow discharge mass spectrometer operated with an argon/hydrogen mixture, J. Am. Soc. Mass Spectrom. 4 (1993) 278–285.

[12] A. Bogaerts, R. Gijbels, Relative sensitivity factors in glow discharge mass spectrometry: the role of charge transfer ionization, J. Anal. At. Spectrom. 11 (1996) 841–847.

[13] A. Bogaerts, R. Gijbels, W.J. Goedheer, Two-dimensional model of a direct current glow discharge: description of the electrons, argon ions and fast argon atoms, Anal. Chem. 68 (1996) 2296–2303.

[14] A. Bogaerts, R. Gijbels, Two-dimensional model of a direct current glow discharge: description of the argon metastable atoms, sputtered atoms and ions, Anal. Chem. 68 (1996) 2676–2685.

[15] G.E. Ice, R.E. Olson, Low energy Ar^+, Kr^+, Xe^++K, Rb, Cs charge-transfer total cross section, Phys. Rev., A 11 (1975) 111–118.

[16] P.A. Amundsen, D.H. Jakubassa, Charge transfer in asymmetric heavy-ion collisions, J. Phys. B: At. Mol. Phys. 13 (1980) L467–L472.

[17] L.J. Dube, A note on the asymptotic behaviour of asymmetric charge transfer theories, J. Phys. B 16 (1983) 1783–1791.

[18] V.N. Ostrvsky, Asymptotic theory of $s \rightarrow p$ charge exchange: extended Demkov model, Phys. Rev., A 49 (1994) 3740–3752.

[19] D.L. Smith, J.H. Futrell, Low energy study of symmetric and asymmetric charge-transfer reactions, J. Chem. Phys. 59 (1973) 463–469.

[20] R. Johnsen, M.T. Leu, M.A. Biondi, Studies of nonresonant charge transfer between atomic ions and atoms, Phys. Rev., A 8 (1973) 1808–1813.

[21] R. Johnsen, J. Macdonald, M.A. Biondi, Thermal energy charge transfer rates for Ne^+, Ne_2^+, Ar^+ and Ar_2^+ ions with Kr and Xe atoms, J. Chem. Phys. 68 (1978) 2991–2992.

[22] I. Dotan, W. Lindinger, B. Rowe, D.W. Fahey, F.C. Fehsenfeld, D.L. Albritton, Rate constants for the reactions of H_2O^+ with NO_2, O_2, NO, C_2H_4, CO, CH_4, and H_2 measured at relative kinetic energies 0.04–2 eV, Chem. Phys. Lett. 72 (1980) 67–70.

[23] M. Durup-Ferguson, H. Bohringer, D.W. Fahey, E.E. Ferguson, Enhancement of charge-transfer reaction rate constants by vibrational excitation at kinetic energies below 1 eV, J. Chem. Phys. 79 (1983) 265–272.

[24] P.B. Farnsworth, J.P. Walters, Excitation processes in an rf boosted, pulsed hollow cathode lamp, Spectrochim. Acta Part B 37 (1982) 773–788.

[25] E.B.M. Steers, R.J. Fielding, Charge transfer excitation processes in the Grimm lamp, J. Anal. At. Spectrom. 2 (1987) 239–244.

[26] E.B.M. Steers, F. Leis, Observations on the use of the microwave-boosted GD lamp and the relevant excitation processes, J. Anal. At. Spectrom. 4 (1989) 199–204.

[27] R.S. Hudson, L.L. Skrumeda, W. Whaling, FeII level populations in a hollow cathode discharge, J. Quant. Spectrosc. Radiat. Transfer 38 (1987) 1–4.

[28] E.B.M. Steers, A.P. Thorne, Application of high-resolution Fourier transform spectrometry to the study of glow discharge sources. Part 1.

Excitation of iron and chromium spectra in a microwave boosted glow discharge source, J. Anal. At. Spectrom. 8 (1993) 309–315.
[29] K. Wagatsuma, K. Hirokawa, Classification of singly ionized iron emission lines in the 160–250 nm wavelength region from the Grimm-type glow discharge plasma, Spectrochim. Acta Part B 51 (1996) 349–374.
[30] E.B.M. Steers, F. Leis, Excitation of the spectra of neutral and singly ionized atoms in the Grimm-type discharge lamp, with and without supplementary microwave excitation, Spectrochim. Acta Part B 46 (1991) 527.
[31] K. Wagatsuma, K. Hirokawa, N. Yamashita, Detection of fluorine emission lines from Grimm-type glow discharge plasmas — use of neon at the plasma gas, Anal. Chim. Acta 324 (1996) 147–154.
[32] K. Wagatsuma, Selective excitation of singly-ionized silver emission lines by Grimm glow discharge plasmas using several different plasma gases, Z. Phys., D At. Mol. Clust. 37 (1996) 231–239.
[33] K. Wagatsuma, K. Hirokawa, Observations of bismuth and lead ionic emission lines excited from Grimm-type glow discharge plasmas with pure neon and neon–argon mixtures, J. Anal. At. Spectrom. 4 (1989) 525–528.
[34] K. Wagatsuma, K. Hirokawa, Observation of singly ionized copper emission lines from a Grimm-type glow discharge with argon–helium gas mixtures in a visible wavelength region, Spectrochim. Acta Part B 48 (1993) 1039–1044.
[35] K. Wagatsuma, Classification of emission lines of the group IIIB elements, Al, Ga, In, excited by Grimm glow discharge plasmas, using several different plasma gases, J. Anal. At. Spectrom. 11 (1996) 957–966.
[36] E.B.M. Steers, Charge transfer excitation in glow discharge sources: the spectra of titanium and copper with neon, argon and krypton as the plasma gas, J. Anal. At. Spectrom. 12 (1997) 1033–1040.
[37] R.B. Shirts, H.P. Parry, P.B. Farnsworth, Anomalous line shapes caused by charge transfer in low-pressure discharges, Spectrochim. Acta Part B 53 (1988) 487–498.
[38] K. Wagatsuma, Y. Danzaki, Non-Boltzmann distribution among energy levels of singly-ionized vanadium in dc glow discharge and rf inductively coupled discharge plasmas, J. Anal. At. Spectrom. 14 (1999) 1727–1730.
[39] K. Wagatsuma, Analytical performance of high-voltage neon plasma in glow discharge optical emission spectrometry, Fresenius J. Anal. Chem. 364 (1999) 780–782.
[40] K. Wagatsuma, H. Honda, Comparative studies on excitation of nickel ionic lines between argon and krypton GD plasmas, Spectrochim. Acta Part B 60 (2005) 1538–1544.
[41] Y. Zhao, G. Horlick, A spectral study of charge transfer and Penning processes for Cu, Zn, Ag and Cd in a glow discharge, Spectrochim. Acta Part B 61 (2006) 660–673.
[42] E.B.M. Steers, P. Smid, Z. Weiss, Asymmetric charge transfer with hydrogen ions — an important factor in the "hydrogen effect" in glow discharge optical emission spectroscopy, Spectrochim. Acta Part B 61 (2006) 414–420.
[43] V.A. Kartazaev, Yu A. Tolmachev, Penning ionization and nonresonant charge exchange in the afterglow of a discharge in a He–Cd mixture, Opt. Spectrosc. 45 (1979) 620–621.
[44] P. Baltayan, J.C. Pebay-Peyroula, N. Sadeghi, Determination of the rate constants for population of the individual Cd^+* levels in thermal Penning and charge transfer reactions of He* (2^3S_1) and He^+ with cadmium, J. Phys. B: At. Mol. Phys. 18 (1985) 3615–3628.
[45] A.R. Turner-Smith, J.M. Green, C.E. Webb, Charge transfer into excited states in thermal energy collisions, J. Phys. B: At. Mol. Phys. 6 (1973) 114–130.
[46] P. Baltayan, J.C. Pebay-Peyroula, N. Sadeghi, Excitation of Zn^+* levels in Penning and charge transfer reactions of He* (2^3S_1) and He^+ with zinc, J. Phys. B: At. Mol. Phys. 19 (1986) 2695–2702.
[47] R. Johnsen, M.A. Biondi, Charge transfer of atomic and molecular rare-gas ions with mercury atoms at thermal energy, J. Chem. Phys. 73 (1980) 5045–5047.
[48] V.N. Ostrovskii, Charge exchange involving ion excitation, Sov. Phys. JETP 57 (1983) 766–769.
[49] A.K. Belyaev, Charge exchange with ion excitation in collisions of helium ions with mercury atoms, J. Phys. B: At. Mol. Phys. 26 (1993) 3877–3890.
[50] H.A. Schuessler, C.H. Holder Jr., O. Chun-Sing, Orbiting charge transfer cross sections between He^+ ions and cesium atoms at near-thermal ion-atom energies, Phys. Rev., A 28 (1983) 1817–1820.
[51] V.A. Kartazaev, Yu.A. Piotrovskii, Yu.A. Tolmachev, Charge exchange and Penning ionization in a pulsed discharge in a mixture of neon and zinc, Opt. Spectrosc. 44 (1978) 362–363.
[52] K.B. Butterfield, D.C. Gerstenberger, T. Shay, W.L. Little, G.J. Collins, Collisional quenching of Xe^+ (^2P) and He 2^3S metastables by calcium and strontium metal vapors, J. Appl. Phys. 49 (1978) 3088–3090.
[53] J.A. Rutherford, D.A. Vroom, Charge transfer cross sections for Hg^+, Xe^+ and Cs^+ in collision with various metals and carbon, J. Chem. Phys. 74 (1981) 434–441.
[54] K.A. Temelkov, N.K. Vuchkov, N.V. Sabotinov, Cross sections and rate constants for charge transfer into excited states, Plasma Process. Polym. 3 (2006) 147–150.
[55] K.A. Temelkov, N.K. Vuchkov, N.V. Sabotinov, Cross sections and rate constants for charge transfer into some Cu^+, Ag^+, and I^+ excited states, Lecture at 2nd International Workshop and Summer School on Plasma Physics, Kiten, Bulgaria, 2006, J. Phys. Conference series (in press).
[56] C.F. Melius, The charge exchange mechanism in metal vapour lasers, J. Phys. B 7 (1974) 1692.
[57] E. Graham IV, M.A. Biondi, R. Johnsen, Spectroscopic studies of the charge-transfer reaction $He^+ + Hg \rightarrow He + (Hg^+)$* at thermal energy, Phys. Rev., A 13 (1976) 965–968.
[58] Y. Tamir, R. Shuker, Thermal energy charge transfer in the Zn–Ar system, J. Appl. Phys. 68 (1990) 5415–5421.
[59] I.G. Ivanov, E.L. Latush, M.F. Sem, Metal Vapour Ion Lasers, John Wiley & Sons, England, 1996.
[60] C.E. Moore, Atomic energy levels, Nat. Stand. Ref. Data Ser., National Bureau Standards, Gaithersburg, MD, USA, vol. I–III, 1971.
[61] C. Beyer, I. Feldmann, D. Gilmour, V. Hoffmann, N. Jakubowski, Development and analytical characterization of a Grimm-type glow discharge ion source operated with high gas flow rates and coupled to a mass spectrometer with high mass resolution, Spectrochim. Acta Part B 57 (2002) 1521–1533.
[62] J.O. Hirschfelder, C.F. Curtiss, B.B. Bird, Molecular Theory of Gases and Liquids, Wiley, New York, 1964.
[63] A. Bogaerts, R. Gijbels, Fundamental aspects and applications of glow discharge spectrometric techniques, Spectrochim. Acta Part B 53 (1998) 1–42.
[64] A. Bogaerts, R. Gijbels, Role of Ar^{2+} and Ar_2^+ ions in a direct current glow discharge: a numerical description, J. Appl. Phys. 86 (1999) 4124–4133.
[65] L.A. Riseberg, W.F. Parks, L.D. Schearer, Penning ionization of Zn and Cd by noble-gas metastable atoms, Phys. Rev., A 8 (1973) 1962–1968.
[66] L. Vriens, Calculation of absolute ionization cross sections of He, He*, He^+, Ne, Ne*, Ne^+, Ar, Ar*, Hg and Hg*, Phys. Lett. 8 (1964) 260–261.
[67] A. Bogaerts, R. Gijbels, J. Vlcek, Collisional-radiative model for an argon glow discharge, J. Appl. Phys. 84 (1998) 121–136.